PHYSICAL REVIEW E **82**, 026108 (2010)

Inferring local dynamics and connectivity of spatially extended systems with long-range links based on steady-state stabilization

Dongchuan Yu[1] and Ulrich Parlitz[2]
[1]*Key Laboratory for NeuroInformation of Ministry of Education, School of Automation Engineering, University of Electronic Science and Technology of China, Chengdu 610054, China*
[2]*Drittes Physikalisches Institut, Georg-August-Universität Göttingen, Friedrich-Hund-Platz 1, D-37077 Göttingen, Germany*
(Received 25 May 2010; revised manuscript received 26 July 2010; published 16 August 2010; corrected 18 August 2010)

A method is presented for system identification of spatially extended systems with structural inhomogeneities of local dynamics and additional long-range links. The proposed identification procedure is based on steady-state stabilization and is illustrated with an inhomogeneous two-dimensional grid of coupled FitzHugh-Nagumo models.

DOI: 10.1103/PhysRevE.82.026108 PACS number(s): 82.40.Ck, 89.75.Fb, 89.75.Kd

I. INTRODUCTION

Many physical and biological dynamical systems are spatially extended and exhibit cooperative wave patterns as well as high-dimensional chaotic attractors. Examples for this kind of complex dynamics are (interacting) spiral waves in brain, heart tissue, or other excitable media [1,2]. In some cases, the structure of these mathematical models can be derived from first principles (e.g., for chemical systems like the Belousov-Zhabotinsky reaction) and only some model parameters have to be determined from experimental data. Often, however, even the structure of the models is not or only partially known and has to be identified using observed data. For both tasks, structure identification and parameter estimation, several methods have been suggested based on nonlinear regression [3], state space reconstruction [4–7], perturbation [8–10], or synchronization [11–14].

To cope with the complexity of the modeling task, the underlying system usually is assumed to be homogeneous. If the system is inhomogeneous in the sense that some parameters vary (slowly) as a function of spatial location, this kind of *parameter inhomogeneity* can be taken into account by including suitable functions of space in the model ansatz. More difficult to identify and to model are *structural inhomogeneities* which occur, for example, due to long-range connections between different (remote) locations in the spatially extended system introducing additional coupling. Such long-range links occur in many natural systems [15–19] and have a strong influence on the dynamics of the full system [20–23]. Therefore, correct identification of these long-range links is of crucial importance for correct modeling.

In this paper, we propose a control based approach to reveal both the local dynamics and the connection topology of systems with additional long-range links. With this method we first stabilize a stationary state (at least in some region) and then exploit the dependence of the equilibrium on control parameters. In this way we obtain all relevant information to identify the underlying dynamics as well as coupling structure. The suggested estimation method can be applied to all systems where the required perturbations are feasible, including coupled circuits, chemical oscillators [24,25], and quantum-dot networks [26].

In order to introduce a general formalism we shall consider in the following spatially extended systems that can (approximately) be described by (large) sets of ordinary differential equations (ODEs). This format occurs naturally for systems with some underlying cell structure and may in general be achieved mathematically by any spatial discretization scheme (e.g., the method of lines [27]). Such spatially discrete system may also be considered as a network, in particular if long-range connections exist in addition to local (diffusive) coupling. From this point of view we shall analyze in the following networks of interacting dynamical systems given by

$$\dot{\boldsymbol{x}}_i = \boldsymbol{f}_i(\boldsymbol{x}_i) + \sum_{j\in V, j\neq i} a_{ij}[\boldsymbol{h}_j(\boldsymbol{x}_{j,\tau_{ij}}) - \boldsymbol{h}_i(\boldsymbol{x}_i)], \tag{1}$$

where dot denotes temporal derivative; $i\in V$ with $V:=\{1,2,\ldots,n\}$ being the set of *vertices*; $\boldsymbol{x}_i=[x_{i1},x_{i2},\ldots,x_{iN}]^\top\in\mathbb{R}^N$ is the state vector of node i; $\boldsymbol{f}_i:\mathbb{R}^N\to\mathbb{R}^N$ describes the local dynamics of node i; and $\boldsymbol{h}_j:\mathbb{R}^N\to\mathbb{R}^N$ is the coupling function from node j to node i. For generality we also include some interaction delay $\tau_{ij}(t)$ which is a function of time and concerns the coupling from node j to node i, with $\boldsymbol{x}_{j,\tau_{ij}}(t):=\boldsymbol{x}_j(t-\tau_{ij})$. We assume that the mappings $\boldsymbol{f}_i$ and $\boldsymbol{h}_j$ are Lipschitzian, that is, there exist positive constants L_{1i} and L_{2j} such that $\|\boldsymbol{f}_i(\boldsymbol{y})-\boldsymbol{f}_i(\boldsymbol{x})\|\le L_{1i}\|\boldsymbol{y}-\boldsymbol{x}\|$ and $\|\boldsymbol{h}_j(\boldsymbol{y})-\boldsymbol{h}_j(\boldsymbol{x})\|\le L_{2j}\|\boldsymbol{y}-\boldsymbol{x}\|$, for all i and j, where $\|.\|$ denotes the Euclidean norm. The parameters a_{ij} are elements of the adjacency matrix $A=(a_{ij})$ describing the topology of the network connections (with $a_{ij}=1$ if there exists a linkage from the node j to the node i, and $a_{ij}=0$ otherwise). The *in-degree* and *out-degree* of node i are defined as $D_i^{in}:=\sum_{k\in V,k\neq i}a_{ik}$ and $D_i^{out}:=\sum_{k\in V,k\neq i}a_{ki}$, respectively. A network is *balanced* if the in-degree of any node is equal to its out-degree. Many real networks are *balanced* such as networks with symmetric connectivity. It should be remarked that if the subscripts i and j represent the ith element and the jth element, respectively, then Eq. (1) can be used to describe very general spatially extended systems.

In the following, we shall suggest a system identification method based on steady-state stabilization. To stabilize a steady state, we add the control signal $\boldsymbol{u}_i$ to the right-hand side of Eq. (1) such that the controlled network [Eq. (1)] is described as

$$\dot{\boldsymbol{x}}_i = \boldsymbol{f}_i(\boldsymbol{x}_i) + \sum_{j\in V, j\neq i} a_{ij}[\boldsymbol{h}_j(\boldsymbol{x}_{j,\tau_{ij}}) - \boldsymbol{h}_i(\boldsymbol{x}_i)] + \boldsymbol{u}_i, \tag{2}$$

where $i \in V$ and $\boldsymbol{u}_i$ are control signals to be designed. For simplicity, here the control signals $\boldsymbol{u}_i$ are designed as

$$\boldsymbol{u}_i = -\theta(\boldsymbol{x}_i - \hat{\boldsymbol{x}}_{is}), \quad i \in V, \tag{3}$$

where control gain θ is a unique value for each node and constants $\hat{\boldsymbol{x}}_{is}$ are used to track the network system to a point of equilibrium.

In the following, we shall focus on the question how to choose control gain θ and parameters $\hat{\boldsymbol{x}}_{is}$ such that: (i) local dynamics $\boldsymbol{f}_i$ can be estimated with high accuracy; and (ii) topology of the network [Eq. (1)] can be identified in terms of an estimation of all elements of the adjacency matrix $A=(a_{ij})$.

This paper is organized as follows. Section II gives the method to identify the local dynamics and connection topology of a quite general network of interacting dynamical systems. After that, we apply in Sec. III the proposed system identification method to a class of spatially extended systems based on this suggested method and illustrate it with an inhomogeneous two-dimensional (2D) grid of coupled FitzHugh-Nagumo models. Finally, we discuss the presented results in Sec. IV.

II. METHOD

A. Steady-state stabilization

The following steady-state control assumption provides the foundation of local dynamics estimation and topology identification.

Assumption 1. There exists a threshold θ_c such that when $\theta > \theta_c$ and any bounded $\hat{\boldsymbol{x}}_{is}$ are used, the system [Eqs. (2) and (3)] is globally driven to a steady-state $(\boldsymbol{x}_{1s}, \boldsymbol{x}_{2s}, \ldots, \boldsymbol{x}_{ns})$, satisfying

$$\sum_{j\in V, j\neq i} a_{ij}[\boldsymbol{h}_j(\boldsymbol{x}_{js}) - \boldsymbol{h}_i(\boldsymbol{x}_{is})] = \theta(\boldsymbol{x}_{is} - \hat{\boldsymbol{x}}_{is}) - \boldsymbol{f}_i(\boldsymbol{x}_{is}), \quad \forall\, i \in V. \tag{4}$$

Remark 1. System [Eqs. (2) and (3)] can be rewritten in a compact form,

$$\dot{\boldsymbol{X}} = \mathcal{H}(\boldsymbol{X}, \boldsymbol{X}_{\tau_{12}}, \ldots, \boldsymbol{X}_{\tau_{ij}}, \ldots) - \theta(\boldsymbol{X} - \boldsymbol{Y}_s), \tag{5}$$

with $\boldsymbol{X}=[\boldsymbol{x}_1^\top, \boldsymbol{x}_2^\top, \ldots, \boldsymbol{x}_n^\top]^\top$ and $\boldsymbol{Y}_s=[\hat{\boldsymbol{x}}_{1s}^\top, \ldots, \hat{\boldsymbol{x}}_{ns}^\top]^\top$. Note that the function $\mathcal{H}$ is Lipschitzian since the functions $\boldsymbol{f}_i$ and $\boldsymbol{h}_{ij}$ are Lipschitzian. Then, it is clear for system [Eq. (5)] with any bounded parameters $\hat{\boldsymbol{x}}_{is}$ that when sufficiently high gain θ is used, there exists a Lyapunov function decreasing along the (steady-state control) error trajectories monotonously; and there exists a solution $(\boldsymbol{x}_{1s}, \boldsymbol{x}_{2s}, \ldots, \boldsymbol{x}_{ns})$ satisfying Eq. (4) by the Theorem 1 in Ref. [28]. Therefore, Assumption 1 is not really a restriction in practice. Furthermore, in the context of pinning control [29,30], our method can be extended to stabilize a network by perturbing only partial nodes of the whole network.

B. Upperbound of tracking errors $\|\boldsymbol{x}_{is} - \hat{\boldsymbol{x}}_{is}\|$

Equation (4) can be rewritten as

$$\boldsymbol{G}(\boldsymbol{X}_s) = \theta(\boldsymbol{X}_s - \boldsymbol{Y}_s), \tag{6}$$

where $\boldsymbol{Y}_s=[\hat{\boldsymbol{x}}_{1s}^\top, \ldots, \hat{\boldsymbol{x}}_{ns}^\top]^\top$, $\boldsymbol{X}_s=[\boldsymbol{x}_{1s}^\top, \ldots, \boldsymbol{x}_{ns}^\top]^\top$, and $\boldsymbol{G}(\boldsymbol{X}_s) =[\boldsymbol{G}_1(\boldsymbol{X}_s)^\top, \ldots, \boldsymbol{G}_n(\boldsymbol{X}_s)^\top]^\top$ with $\boldsymbol{G}_i(\boldsymbol{X}_s)=\boldsymbol{f}_i(\boldsymbol{x}_{is}) + \sum_{j\in V, j\neq i} a_{ij}[\boldsymbol{h}_j(\boldsymbol{x}_{js}) - \boldsymbol{h}_i(\boldsymbol{x}_{is})]$. Then one has

$$\begin{aligned}
\|\boldsymbol{X}_s - \boldsymbol{Y}_s\|^2 &= \left\| \frac{1}{\theta}(\boldsymbol{X}_s - \boldsymbol{Y}_s)^\top \boldsymbol{G}(\boldsymbol{X}_s) \right\| \\
&\leq \frac{1}{\theta}\|(\boldsymbol{X}_s - \boldsymbol{Y}_s)^\top \boldsymbol{G}(\boldsymbol{Y}_s)\| \\
&\quad + \frac{1}{\theta}\|(\boldsymbol{X}_s - \boldsymbol{Y}_s)^\top [\boldsymbol{G}(\boldsymbol{X}_s) - \boldsymbol{G}(\boldsymbol{Y}_s)]\| \\
&\leq \frac{1}{\theta}\|\boldsymbol{X}_s - \boldsymbol{Y}_s\| \times \|\boldsymbol{G}(\boldsymbol{Y}_s)\| + \frac{1}{\theta}\sum_i L_{1i}\|\boldsymbol{x}_{is} - \hat{\boldsymbol{x}}_{is}\|^2 \\
&\quad + \frac{1}{\theta}\sum_i \|\boldsymbol{x}_{is} - \hat{\boldsymbol{x}}_{is}\| \sum_{j\in V, j\neq i} a_{ij} L_{2i} \|\boldsymbol{x}_{is} - \hat{\boldsymbol{x}}_{is}\| \\
&\quad + \frac{1}{\theta}\sum_i \|\boldsymbol{x}_{is} - \hat{\boldsymbol{x}}_{is}\| \sum_{j\in V, j\neq i} a_{ij} L_{2j} \|\boldsymbol{x}_{js} - \hat{\boldsymbol{x}}_{js}\| \\
&\leq \frac{1}{\theta}\|\boldsymbol{X}_s - \boldsymbol{Y}_s\| \times \|\boldsymbol{G}(\boldsymbol{Y}_s)\| + \frac{L_G}{\theta}\|\boldsymbol{X}_s - \boldsymbol{Y}_s\|^2
\end{aligned}$$

where $L_G=\max_i[L_{1i} + D_i^{in} L_{2i} + \frac{1}{2}\sum_{j\in V, j\neq i}(a_{ij}L_{2j} + a_{ji}L_{2i})]$.

It follows that when $\theta > L_G$ is used, one obtains

$$\|\boldsymbol{X}_s - \boldsymbol{Y}_s\| \leq \frac{\|\boldsymbol{G}(\boldsymbol{Y}_s)\|}{\theta - L_G}. \tag{7}$$

C. Identification of local dynamics

We now show that steady state Eq. (4) can be used to estimate the functions $\boldsymbol{f}_i$ (describing the local dynamics) of *balanced networks*, if the equilibrium points $\boldsymbol{x}_{is}$ are measurable. Our idea is very simple and is based on the following facts: (i) the sum of the left hand side of Eq. (4) over node index i is zero for *balanced networks*; and (ii) since $\boldsymbol{f}_i$ is Lipschitzian [i.e., $\|\boldsymbol{f}_i(\boldsymbol{y}) - \boldsymbol{f}_i(\boldsymbol{x})\| \leq L_{1i}\|\boldsymbol{y} - \boldsymbol{x}\|$], $\theta(\boldsymbol{x}_{is} - \hat{\boldsymbol{x}}_i)$ dominates the term $\theta(\boldsymbol{x}_{is} - \hat{\boldsymbol{x}}_i) - \boldsymbol{f}_i(\boldsymbol{x}_{is}) + \boldsymbol{f}_i(\hat{\boldsymbol{x}}_i)$, when $\theta \gg L_{1i}$ is used. The detailed analysis is the following.

We sum Eq. (4) over node index i and obtain

$$\mathbf{F} = \sum_{i\in V}\sum_{j\in V, j\neq i} a_{ij}[\boldsymbol{h}_j(\boldsymbol{x}_{js}) - \boldsymbol{h}_i(\boldsymbol{x}_{is})] = \sum_{i\in V} \theta(\boldsymbol{x}_i - \hat{\boldsymbol{x}}_{is}) - \boldsymbol{f}_i(\boldsymbol{x}_{is}). \tag{8}$$

If the diffusion operator represents a *balanced network*, then the left hand side of Eq. (8) vanishes,

$$\begin{aligned}\mathbf{F} &= \sum_{i\in V}\sum_{j\in V, j\neq i} a_{ij}\boldsymbol{h}_j(\boldsymbol{x}_{js}) - \sum_{i\in V}\boldsymbol{h}_i(\boldsymbol{x}_{is})\left(\sum_{j\in V, j\neq i} a_{ij}\right)\\ &= \sum_{j\in V}\boldsymbol{h}_j(\boldsymbol{x}_{js})\left(\sum_{i\in V, i\neq j} a_{ij}\right) - \sum_{j\in V}\boldsymbol{h}_j(\boldsymbol{x}_{js})\left(\sum_{i\in V, i\neq j} a_{ji}\right)\\ &= \sum_{j\in V}\boldsymbol{h}_j(\boldsymbol{x}_{js})\left(\sum_{i\in V, i\neq j} a_{ij} - \sum_{i\in V, i\neq j} a_{ji}\right) = \mathbf{0}.\end{aligned}$$

Therefore, Eq, (8) yields

$$\begin{aligned}\mathbf{0} &= \sum_{i\in V}[\theta(\boldsymbol{x}_{is}-\hat{\boldsymbol{x}}_i) - \boldsymbol{f}_i(\boldsymbol{x}_{is})]\\ &= \sum_{i\in V}[\theta(\boldsymbol{x}_{is}-\hat{\boldsymbol{x}}_i) - \boldsymbol{f}_i(\boldsymbol{x}_{is}) + \boldsymbol{f}_i(\hat{\boldsymbol{x}}_i) - \boldsymbol{f}_i(\hat{\boldsymbol{x}}_i)],\end{aligned}$$

resulting in

$$\sum_{i\in V}\boldsymbol{f}_i(\hat{\boldsymbol{x}}_i) = \sum_{i\in V}[\theta(\boldsymbol{x}_{is}-\hat{\boldsymbol{x}}_i) - \boldsymbol{f}_i(\boldsymbol{x}_{is}) + \boldsymbol{f}_i(\hat{\boldsymbol{x}}_i)].$$

Because $\boldsymbol{f}_i$ is Lipschitzian (i.e., $\|\boldsymbol{f}_i(\boldsymbol{y})-\boldsymbol{f}_i(\boldsymbol{x})\| \leq L_{1i}\|\boldsymbol{y}-\boldsymbol{x}\|$, where L_{1i} denotes the Lipschitz constant of $\boldsymbol{f}_i$), we obtain for $\theta \gg L_{1i}$

$$\sum_{i\in V}\boldsymbol{f}_i(\hat{\boldsymbol{x}}_i) \approx \sum_{i\in V}\theta(\boldsymbol{x}_{is}-\hat{\boldsymbol{x}}_i). \tag{9}$$

Now we assume that a data-pair $(\boldsymbol{c}_k, \boldsymbol{f}_k(\boldsymbol{c}_k))$ is known for all k (for example, $\boldsymbol{c}_k=\mathbf{0}$ and $\boldsymbol{f}_k(\mathbf{0})=\mathbf{0}$). Then, for *any* given i, setting $\hat{\boldsymbol{x}}_k=\boldsymbol{c}_k$ for $k\neq i$ in Eq. (9), we obtain

$$\hat{\boldsymbol{f}}_i(\hat{\boldsymbol{x}}_i) = \sum_{k\in V}\theta(\boldsymbol{x}_{ks}-\hat{\boldsymbol{x}}_k) - \sum_{k\in V, k\neq i}\boldsymbol{f}_k(\boldsymbol{c}_k), \tag{10}$$

where all $\boldsymbol{x}_{ks}$ are functions of $\hat{\boldsymbol{x}}_i$ and $\hat{\boldsymbol{f}}_i$ is an estimate of $\boldsymbol{f}_i$. In this way we can approximate $\boldsymbol{f}_i$ by $\hat{\boldsymbol{f}}_i$ by gradually changing $\hat{\boldsymbol{x}}_i$ in a desired range to scan the underlying functional relation. Even if $\Gamma=\sum_{k\in V, k\neq i}\boldsymbol{f}_k(\boldsymbol{c}_k)$ is unknown, we can at least estimate the shifted mapping $\hat{\boldsymbol{f}}_i+\Gamma$.

In order to obtain an approximated (nonshifted) mapping $\boldsymbol{f}_i$, one has to estimate Γ. To do so, particular function values $\boldsymbol{f}_k(\boldsymbol{c}_k)$ have to be known, only, where the $\boldsymbol{c}_k$ for all $k\neq i$ can be chosen freely. In practice, if each node can be separated from the full system by some proper (physical or chemical) operations, the equilibrium point of each individual node can be stabilized and thereby identified by delayed feedback control [31,32]. In this case, one may exploit the values of functions $\boldsymbol{f}_k$ at the equilibrium point.

On the other hand, if only Γ is unknown then one may use the model which has been detected so far (i.e., the local dynamics $\boldsymbol{f}_i$ and the coupling) and use it for short time prediction of the measured time series of the observable variables. One may vary Γ and plot the (averaged) prediction error versus Γ. At the "right Γ" there should be a (global) minimum. Based on the above principle, one can also estimate the value of Γ.

D. Topology identification

We now show that all elements of the adjacency matrix $A=(a_{ij})$ can be estimated by two pinnings with control signals [Eq. (3)] with different $\hat{\boldsymbol{x}}_{ks}$. For the ℓth pinning, the control signals actually read

$$\boldsymbol{u}_i^{(\ell)} = -\theta(\boldsymbol{x}_i^{(\ell)} - \hat{\boldsymbol{x}}_{is}^{(\ell)}), \quad i\in V, \quad \ell\in\{1,2\} \tag{11}$$

with

$$\hat{\boldsymbol{x}}_{ks}^{(\ell)} = \begin{cases} \boldsymbol{z}_j^{(\ell)}, & \text{for } k=j,\\ \mathbf{0}, & \text{otherwise}.\end{cases} \tag{12}$$

Here and hereafter the superscript $^{(\ell)}$ denotes the ℓth steady-state control.

One can easily conclude from Assumption 1 that when $\theta>\theta_c$ is used, the network can be driven to a steady state for each pinning. For the ℓth pinning, the steady state Eq. (4) becomes

$$a_{ij}[\boldsymbol{h}_j(\boldsymbol{z}_j^{(\ell)}) - \boldsymbol{h}_i(\mathbf{0})] + \psi_i - \boldsymbol{\Delta}_i^{(\ell)} = \theta\boldsymbol{x}_{is}^{(\ell)}, \quad \forall\, i\in V\setminus\{j\}. \tag{13}$$

where $\psi_i=\sum_{k\in V, k\neq i,j} a_{ik}[\boldsymbol{h}_k(\mathbf{0})-\boldsymbol{h}_i(\mathbf{0})]+\boldsymbol{f}_i(\mathbf{0})$; and

$$\begin{aligned}\boldsymbol{\Delta}_i^{(\ell)} &:= \boldsymbol{f}_i(\hat{\boldsymbol{x}}_{is}^{(\ell)}) - \boldsymbol{f}_i(\boldsymbol{x}_{is}^{(\ell)})\\ &\quad + \sum_{j\in V, j\neq i} a_{ij}[\boldsymbol{h}_j(\hat{\boldsymbol{x}}_{js}^{(\ell)}) - \boldsymbol{h}_j(\boldsymbol{x}_{js}^{(\ell)}) - \boldsymbol{h}_i(\hat{\boldsymbol{x}}_{is}^{(\ell)}) + \boldsymbol{h}_i(\boldsymbol{x}_{is}^{(\ell)})].\end{aligned} \tag{14}$$

Subtracting Eq. (13) for $\ell=1$ from that for $\ell=2$ yields for $i\in V\setminus\{j\}$

$$a_{ij}\rho_j + \varpi_{ij} = \theta\beta_i, \tag{15}$$

where

$$\begin{aligned}\rho_j &= \boldsymbol{h}_j(\boldsymbol{z}_j^{(2)}) - \boldsymbol{h}_j(\boldsymbol{z}_j^{(1)}),\\ \varpi_{ij} &= \boldsymbol{\Delta}_i^{(1)} - \boldsymbol{\Delta}_i^{(2)},\\ \beta_{ij} &= \boldsymbol{x}_{is}^{(2)} - \boldsymbol{x}_{is}^{(1)}.\end{aligned} \tag{16}$$

We now show that the above Eq. (15) can be applied for topology identification, if sufficiently high θ is used. This method is based on the following facts: (i) the upper bound of $\|\boldsymbol{\Delta}_i^{(\ell)}\|$ decreases with θ since $\boldsymbol{f}_i$ and $\boldsymbol{h}_j$ are Lipschitzian and the upper bound of the tracking error $\|\boldsymbol{X}_s-\boldsymbol{Y}_s\|$ decreases with the control gain θ [cf. Eq. (7)]; and (ii) for a given j, the values of $a_{ij}\rho_j$ corresponding to $a_{ij}=1$ are distinguishable from that corresponding to $a_{ij}=0$, for all $i\in V\setminus\{j\}$. The detailed analysis is the following.

Since the vector Eq. (15) actually contains N equations, we can estimate the elements a_{ij} from any one equation, say the mth equation of Eq. (15), given by

$$a_{ij}\eta_j + \lambda_{ij} = \theta S_{ij}^{\Delta}, \quad \forall\, i\in V\setminus\{j\}, \tag{17}$$

with

$$\eta_j = \rho_j^m, \quad \lambda_{ij} = \varpi_{ij}^m, \quad S_{ij}^{\Delta} = \beta_{ij}^m, \tag{18}$$

wherein the superscript ^{m} denotes the mth element of vector.

It follows that $\forall i\in V\setminus\{j\}$,

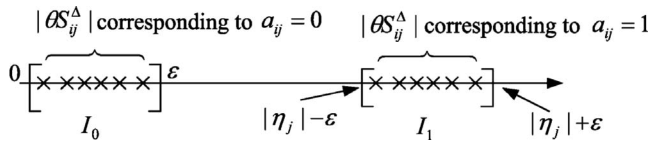

FIG. 1. Diagram of set $\mathbf{I}_0$ containing all elements $|\theta S_{ij}^{\Delta}|$ corresponding to $a_{ij}=0$ and set $\mathbf{I}_1$ containing all elements $|\theta S_{ij}^{\Delta}|$ corresponding to $a_{ij}=1$.

$$\theta S_{ij}^{\Delta}=\begin{cases}\eta_j+\lambda_{ij}, & \text{for } a_{ij}=1,\\ \lambda_{ij}, & \text{for } a_{ij}=0.\end{cases} \tag{19}$$

This implies that if one can distinguish the values $\eta_j+\lambda_{ij}$ and λ_{ij}, then one can identify the element a_{ij} correctly.

On the other hand, it is clear that

$$\begin{aligned}\|\boldsymbol{\Delta}_i^{(\ell)}\| &\le L_{1i}\|\hat{\boldsymbol{x}}_{is}^{(\ell)}-\boldsymbol{x}_{is}^{(\ell)}\| \\ &\quad+\sum_{j\in V,j\neq i}a_{ij}(L_{2j}\|\hat{\boldsymbol{x}}_{js}^{(\ell)}-\boldsymbol{x}_{js}^{(\ell)}\|+L_{2i}\|\hat{\boldsymbol{x}}_{is}^{(\ell)}-\boldsymbol{x}_{is}^{(\ell)}\|) \\ &\le\left[L_{1i}+\sum_{j\in V,j\neq i}a_{ij}(L_{2j}+L_{2i})\right]\frac{\|\boldsymbol{G}(\boldsymbol{Y}_s^{(\ell)})\|}{\theta-L_G} \\ &\le\frac{\Omega_{\max}\|\boldsymbol{G}(\boldsymbol{Y}_s^{(\ell)})\|}{\theta-L_G}\end{aligned} \tag{20}$$

where Eq. (7) and $a_{ij}\ge 0$ for all $i\neq j$ are used; $\boldsymbol{Y}_s^{(\ell)}=[(\hat{\boldsymbol{x}}_{1s}^{(\ell)})^{\top},(\hat{\boldsymbol{x}}_{2s}^{(\ell)})^{\top},\ldots,(\hat{\boldsymbol{x}}_{ns}^{(\ell)})^{\top}]^{\top}$; and

$$\Omega_{\max}:=\max_{i\in V}\left\{\left[L_{1i}+\sum_{j\in V,j\neq i}a_{ij}(L_{2j}+L_{2i})\right]\right\}. \tag{21}$$

It follows from definitions (16) and (18) that

$$|\lambda_{ij}|\le\varepsilon \tag{22}$$

where

$$\varepsilon=\frac{\Omega_{\max}[\|\boldsymbol{G}(\boldsymbol{Y}_s^{(2)})\|+\|\boldsymbol{G}(\boldsymbol{Y}_s^{(1)})\|]}{\theta-L_G}. \tag{23}$$

One can conclude from Eqs. (19) and (22) that $\forall i\in V\backslash\{j\}$

$$|\theta S_{ij}^{\Delta}|\in\begin{cases}[0,\varepsilon], & \text{for } a_{ij}=0,\\ [|\eta_j|-\varepsilon,|\eta_j|+\varepsilon], & \text{for } a_{ij}=1.\end{cases} \tag{24}$$

This implies that all values $|\theta S_{ij}^{\Delta}|$ can be divided into two sets $\mathbf{I}_0\subset[0,\varepsilon]$ containing all elements $|\theta S_{ij}^{\Delta}|$ corresponding to $a_{ij}=0$ and $\mathbf{I}_1\subset[|\eta_j|-\varepsilon,|\eta_j|+\varepsilon]$ containing all elements $|\theta S_{ij}^{\Delta}|$ corresponding to $a_{ij}=1$, as shown in Fig. 1. As a result, if one can discriminate sets $\mathbf{I}_0$ and $\mathbf{I}_1$, then one can identify all elements a_{ij} of the connectivity matrix.

One can easily find from Fig. 1 that if

$$|\eta_j|>3\varepsilon$$

or equivalently

$$\theta>\frac{3\Omega_{\max}[\|\boldsymbol{G}(\boldsymbol{Y}_s^{(2)})\|+\|\boldsymbol{G}(\boldsymbol{Y}_s^{(1)})\|]}{|\eta_j|}+L_G, \tag{25}$$

then the distance between sets $\mathbf{I}_0$ and $\mathbf{I}_1$ is larger than the maximal value of set $\mathbf{I}_0$ [33]. On the other hand, it is easy to see from Eq. (23) that the value of ε decreases with θ. As a result, the critical point of set $\mathbf{I}_0$ (namely the point with the maximal value of set $\mathbf{I}_0$) decreases with θ but that of set $\mathbf{I}_1$ (namely, the point with the minimal value of set $\mathbf{I}_1$) increases with θ.

To summarize the above analysis, if condition (25) is fulfilled, then one can distinguish sets $\mathbf{I}_0$ and $\mathbf{I}_1$ by the following *set discrimination based topology identification algorithm* (SDTIA):

Step 1. Calculate elements θS_{ij}^{Δ} for all $i\neq V\backslash\{j\}$ using definition (17).

Step 2. Order (or arrange) all elements $|\theta S_{ij}^{\Delta}|$ in an ascending sequence and obtain a new sequence $\{b_i\}$ with $b_i\le b_{i+1}$ for $i=1,2,\ldots,n-2$.

Step 3. Determine the critical point sequence number i_c of set $\mathbf{I}_1$ by the rules: (i) $b_i-b_1\ge 2(b_{i_c}-b_1)$, $\forall i>i_c$; (ii) b_{i_c} decreases but b_{i_c+1} increases with θ.

Remark 2. Estimating topology by SDTIA actually includes the following five steps: (i) driving the network to steady-state twice by the control signals [Eq. (11)]; (ii) measuring the corresponding steady-state response $(\boldsymbol{x}_{1s}^{(\ell)},\boldsymbol{x}_{2s}^{(\ell)},\ldots,\boldsymbol{x}_{ns}^{(\ell)})$ of each node for each pinning; (iii) calculating elements $|\theta S_{ij}^{\Delta}|$ given by Eq. (18) for all $i\in V\backslash\{j\}$; (iv) arranging all elements $|\theta S_{ij}^{\Delta}|$ in an ascending sequence and obtaining a new sequence $\{b_i\}$ with $b_i\le b_{i+1}$ for $i=1,2,\ldots,n-2$; and (v) estimating all connections starting from node j by determining the critical point sequence number i_c in the light of the rule described in SDTIA.

Remark 3. There exists a critical value θ_c such that if $\theta>\theta_c$, the maximal value of set $\mathbf{I}_0$ decreases with θ; the minimal value of set $\mathbf{I}_1$ increases with θ. This feature can also be applied to identify both sets $\mathbf{I}_0$ and $\mathbf{I}_1$. In practice, one can first choose a small control gain θ and then increase θ gradually until the distance between sets $\mathbf{I}_0$ and $\mathbf{I}_1$ is larger than the maximal value of set $\mathbf{I}_0$. In this way one can always find a proper control gain θ. Furthermore the performance of topology identification also depends on the value of η_j. Many numerical experiments have shown that both the maximal value of set $\mathbf{I}_0$ and the minimal value of set $\mathbf{I}_1$ increase almost linearly with $|\eta_j|$, but the former has much smaller increasing rate than the latter and thereby the distance between sets $\mathbf{I}_0$ and $\mathbf{I}_1$ is almost linearly increased with θ. This feature can also be applied to topology identification. In practice, one may apply the trial-and-error method for choosing a proper η_j such that the distance between sets $\mathbf{I}_0$ and $\mathbf{I}_1$ is larger than the maximal value of set $\mathbf{I}_0$.

III. EXAMPLE: COUPLED FITZHUGH-NAGUMO-SYSTEMS

As an example to illustrate the identification methods introduced in Sec. II, we shall consider now an inhomogeneous spatiotemporal system given by a 2D grid of coupled ODEs. The ODEs describe the local dynamics of coupled elements on a 2D grid $G=[1,\ldots,N_1]\times[1,\ldots,N_2]$ (with von Neumann boundary conditions) where the state evolution of each node $(i,j)\in G$ is governed by

$$\dot{x}_{i,j} = f_{i,j}(x_{i,j}, y_{i,j}) + D_{i,j}, \tag{26}$$

$$\dot{y}_{i,j} = g_{i,j}(x_{i,j}, y_{i,j}). \tag{27}$$

The diffusion operator

$$D_{i,j} = \sum_{(k_1,k_2)\neq(i,j)} a_{(i,j),(k_1,k_2)}[h_{k_1,k_2}(x_{k_1,k_2}) - h_{i,j}(x_{i,j})] \tag{28}$$

is defined in terms of a general coupling function $h_{i,j}$ and acts here on the first variable x only. Generalizations to more complex diffusion operators (acting on all state variables or/and appearing in all evolution equations) are straightforward. The parameters $a_{(i,j),(k_1,k_2)}$ describe the connectivity of the medium (with $a_{(i,j),(k_1,k_2)}=1$ if there exists a connection from site (k_1,k_2) to site (i,j), and $a_{(i,j),(k_1,k_2)}=0$ otherwise).

The local dynamics of the system of coupled ODEs is given by FitzHugh-Nagumo (FHN) models [21]

$$f_{i,j} = (x_{i,j} - x_{i,j}^3/3 - y_{i,j})/\epsilon_{i,j}, \tag{29}$$

$$g_{i,j} = \epsilon_{i,j}(b_{i,j}x_{i,j} - \gamma_{i,j}y_{i,j} + \beta_{i,j}), \tag{30}$$

with $\epsilon_{i,j}$, $\beta_{i,j}$, $\gamma_{i,j}$, and $b_{i,j}$ uniformly distributed in [0.08 0.18], [0.6 0.8], [0.4 0.6], and [0.8 1.2], respectively. In the following, $N_1=N_2=100$ and $h_{i,j}(x)\equiv x$. This system of ODEs describes a reaction-diffusion system modeling excitable and oscillatory media. Without long-range connections the diffusion is given by an approximation $[x_{i-1,j}+x_{i+1,j}+x_{i,j-1}+x_{i,j+1}-4x_{i,j}]/\Delta^2$ of the differential operator $\nabla^2 x$ where Δ denotes the step size of spatial discretization [34]. In addition to the nearest neighbors coupling further long-range random connections between remote elements are established with probability $p_c=0.01$ in order to render the system structurally inhomogeneous, as shown in Fig. 2(a). In this way we obtain an inhomogeneous spatiotemporal system with small-world [20–23] coupling structure that has to be identified, and its spatiotemporal dynamical behavior is plotted in Fig. 2(b). It should be remarked that this system can be considered as a particular example of system [Eq. (1)]. Therefore, the suggested identification method using steady-state stabilization is applicable to system [Eqs. (26)–(30)].

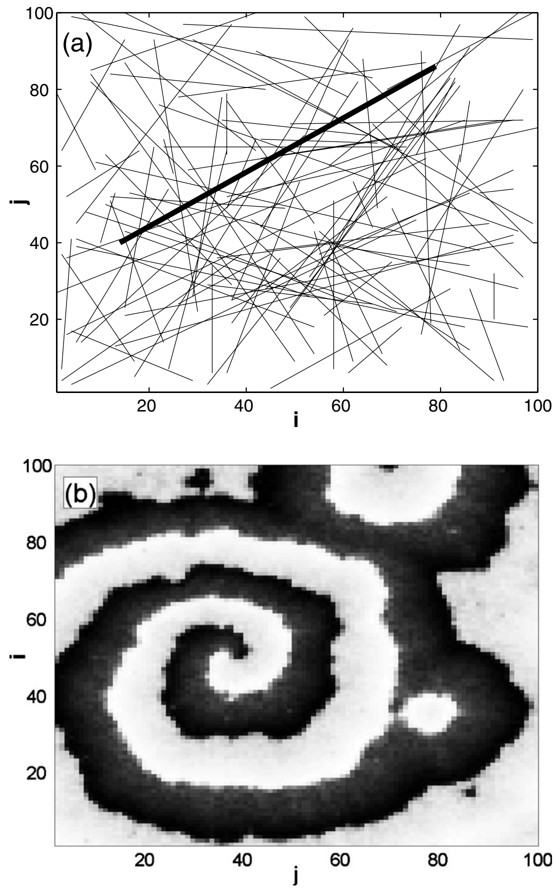

FIG. 2. (a) Lines represent long-range random connections between remote sites with probability $p_c=0.01$ where the highlighted (thicker) line shows the connection from site (79,86) to site(14,40). (b) Snap shot of excitation waves of the inhomogeneous FHN medium [Eqs. (26)–(30)] showing $x_{i,j}(t)$ in grayscale.

A. Steady-state stabilization

To stabilize a steady state in some region $\mathbf{R}_c$, we add the control terms

$$u_{i,j}^{(1)} = -\theta(x_{ij} - w_{i,j}^{(1)}), \quad (i,j) \in \mathbf{R}_c \subseteq G,$$

$$u_{i,j}^{(2)} = -\theta(y_{ij} - w_{i,j}^{(2)}), \quad (i,j) \in \mathbf{R}_c \subseteq G, \tag{31}$$

to the right-hand side of Eqs. (26) and (27), respectively. Here $\mathbf{R}_c \subseteq G$ is the set of sites accessible, and the uniform control gain θ and constants $w_{i,j}^{(1)}$ and $w_{i,j}^{(2)}$ will be specified below.

Experimentally, a computer may sample and record simultaneously the measurable variables of all sites in $\mathbf{R}_c$ through a multichannel analog-to-digital converter and generate the control signals [Eq. (31)] by a multichannel digital-to-analog converter, which will be fed (or injected) back to the system.

It has been shown above that system [Eqs. (26)–(28)] can be driven to some stationary state $(\dot{x}_{i,j}=\dot{y}_{i,j}=0)$ using control signal [Eq. (31)]. This control can also be restricted to some local areas to drive only some part(s) of the extended system to stationary dynamics, as illustrated in Fig. 3.

B. Local dynamics estimation

We first show that steady-state stabilization is applicable to local dynamics estimation. In this case, Eqs. (26)–(28) under the control signal [Eq. (31)] reduce to

$$f_{i,j}(\tilde{x}_{i,j}, \tilde{y}_{i,j}) = -D_{i,j} + \theta(\tilde{x}_{i,j} - w_{i,j}^{(1)}), \tag{32}$$

$$g_{i,j}(\tilde{x}_{i,j}, \tilde{y}_{i,j}) = \theta(\tilde{y}_{i,j} - w_{i,j}^{(2)}). \tag{33}$$

Here and hereafter, the superscript denotes the corresponding steady-state response.

Functions $g_{i,j}$ can be estimated by Eq. (33), if one first changes parameters $w_{i,j}^{(1)}$ and $w_{i,j}^{(2)}$ and then obtains the data-pair sets $\{(\tilde{x}_{i,j}, \tilde{y}_{i,j}), \theta(\tilde{y}_{i,j} - w_{i,j}^{(2)})\}$ representing the functional

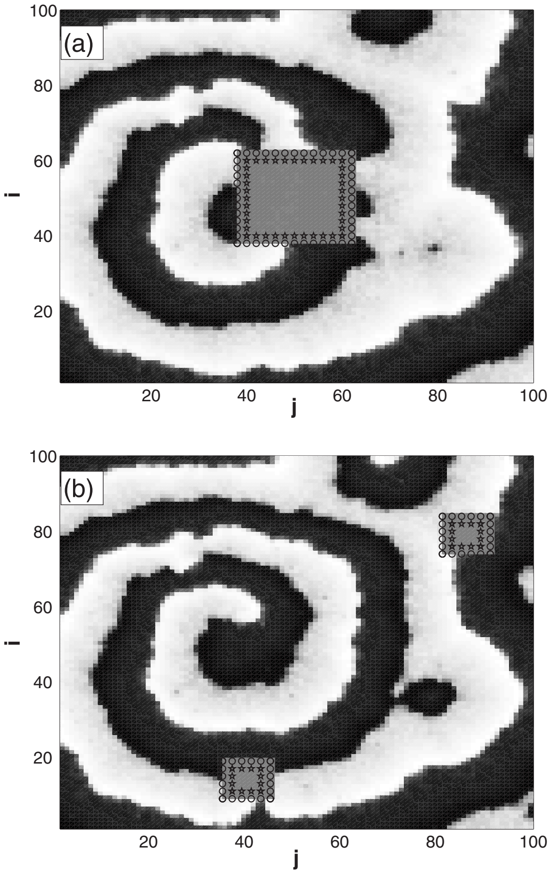

FIG. 3. Snap shot of excitation waves of the (controlled) FHN medium (26)–(30) showing $x_{i,j}(t)$ in grayscale, when control signal [Eq. (31)] is used, with: (a) $\theta=100$, $\mathbf{R}_c=[38,39,\ldots,62]\times[38,39,\ldots,62]$ (circle frame), $w_{i,j}^{(1)}=w_{i,j}^{(2)}=0$; and (b) $\theta=100$, $u_{i,j}^{(2)}=0$, $\mathbf{R}_c=[74,\ldots,84]\times[81,\ldots,91]\cup[9,\ldots,19]\times[35,\ldots,45]$ (circle frames), $w_{i,j}^{(1)}=w_{i,j}^{(2)}=0$. A region $\mathbf{R}_s$ (star frame(s)) (a little bit smaller than $\mathbf{R}_c$) is driven to some stationary state.

relation of $g_{i,j}$. To estimate the functions $f_{i,j}$, we sum Eq. (32) over element index (i,j) and obtain:

$$\sum_{(i,j)} f_{i,j}(\tilde{x}_{i,j},\tilde{y}_{i,j}) = -\sum_{(i,j)} D_{i,j} + \sum_{(i,j)} \theta(\tilde{x}_{i,j} - w_{i,j}^{(1)}). \quad (34)$$

As shown in Sec. II B, for balanced spatiotemporal systems, the first term of the right-hand side of Eq. (8) vanishes. Therefore, Eq. (34) yields

$$f_{i,j}(\tilde{x}_{i,j},\tilde{y}_{i,j}) = \theta(\tilde{x}_{i,j} - w_{i,j}^{(1)}) - \Gamma + \sum_{(k_1,k_2)\neq(i,j)} [\theta(\tilde{x}_{k_1,k_2} - w_{k_1,k_2}^{(1)}) + f_{k_1,k_2}(w_{k_1,k_2}^{(1)},w_{k_1,k_2}^{(2)}) - f_{k_1,k_2}(\tilde{x}_{k_1,k_2},\tilde{y}_{k_1,k_2})], \quad (35)$$

where $\Gamma=\Sigma_{(k_1,k_2)\neq(i,j)} f_{k_1,k_2}(w_{k_1,k_2}^{(1)},w_{k_1,k_2}^{(2)})$.

It has been shown in Sec. II B that if the control gain θ is large enough, then

$$f_{i,j}(\tilde{x}_{i,j},\tilde{y}_{i,j}) + \Gamma \approx \sum_{(k_1,k_2)} \theta(\tilde{x}_{k_1,k_2} - w_{k_1,k_2}^{(1)}), \quad (36)$$

and the value of $f_{i,j}+\Gamma$ at the resulting steady-state response $(\tilde{x}_{i,j},\tilde{y}_{i,j})$ (depending on the values of θ and parameters $w_{i,j}^{(1)}$

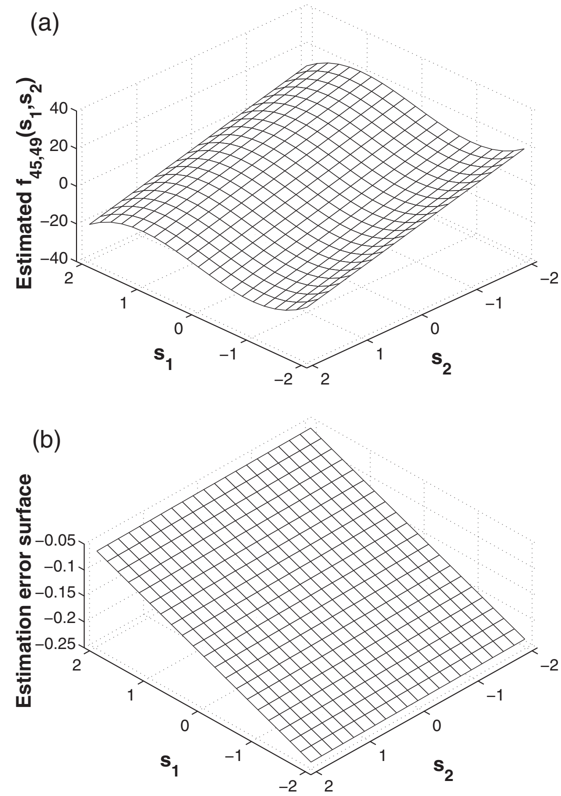

FIG. 4. Estimation of local dynamics at site (45,49) of the FHN medium [Eqs. (26)–(30)] where the unit of the quantity being plotted in each axis is arbitrary. (a) Estimated $f_{45,49}$ and (b) estimation errors caused by the approximation leading to Eq. (36). To obtain this result, we scanned with $(w_{ij}^{(1)},w_{ij}^{(2)})$ the area $[-2\ 2]\times[-2\ 2]$ with step size 0.2 and measured the resulting steady state (s_1,s_2).

and $w_{i,j}^{(2)}$) can be estimated. In this way, function $f_{i,j}+\Gamma$ can be approximated by first performing a series of steady-state controls and then achieving a series of data-pairs $\{(\tilde{x}_{i,j},\tilde{y}_{i,j}),\Sigma_{(k_1,k_2)}\theta(\tilde{x}_{k_1,k_2}-w_{k_1,k_2}^{(1)})\}$ to represent the approximated functional relation, where we fix parameters $w_{i,j}^{(1)}$ and $w_{i,j}^{(2)}$ (with freely chosen values) for all $(k_1,k_2)\neq(i,j)$ and we scan the values of $(w_{i,j}^{(1)},w_{i,j}^{(2)})$ on a 2D grid with suitable step size. If the constant Γ is known [35], we can estimate the function $f_{i,j}$.

If stabilizing the full system is not possible (or allowed), a sequence of measurements may be performed where only small regions are stabilized and the remaining system is not controlled. In this way one may identify the whole system structure by collecting and combining information obtained from many small regions. This approach is illustrated in Fig. 3, where some local area $\mathbf{R}_s$ is driven to a steady state by applying control to a slightly larger region $\mathbf{R}_c$. This example shows that the suggested technique is robust and can be applied to estimate the local dynamics of sites in any subnetwork $\mathbf{R}_s$ where remaining regions of the system are not perturbed. As a representative example Fig. 4(a) shows the estimation for $f_{45,49}$ which is recovered with high accuracy [see errors in Fig. 4(b)], where $\theta=800$ and $w_{k_1,k_2}^{(1)}=w_{k_1,k_2}^{(2)}\equiv 0$ for all $(k_1,k_2)\neq(45,49)$ which in combination with Eq. (29)

leads to $\Gamma=0$ and hence the nonshifted $f_{45,49}$ can be estimated using Eq. (36).

C. Connection topology estimation

We now show how to apply SDTIA for topology estimation of the spatially extended system [Eqs. (26)–(30)] as a representative example, and restrict ourselves to the case in which only the x-variable is accessible (i.e., $u_{i,j}^{(2)}=0$) [see Fig. 3(b)] and show that driving the medium to two different stationary states by local control signals [Eq. (31)] enables to infer connections starting from any element $(m,n)\in\mathbf{R}_s$. In this case, Eq. (32) still holds, as illustrated in Fig. 3(b). For the ℓth stationary state control, we set

$$w_{k_1,k_2}^{(1)}=\begin{cases}\eta_{m,n}^{(\ell)}, & \text{for } (k_1,k_2)=(m,n),\\ 0, & \text{otherwise},\end{cases} \tag{37}$$

where $\ell\in\{1,2\}$. Then we obtain from Eq. (32) that

$$a_{(i,j),(m,n)}[h_{m,n}(\eta_{m,n}^{(\ell)})-h_{i,j}(0)]+\Phi_{i,j}-\Delta_{i,j}^{(\ell)}=\theta\tilde{x}_{i,j}^{(\ell)}, \tag{38}$$

where the superscript $^{(\ell)}$ represents the ℓth control; and

$$\Phi_{i,j}=f_{i,j}(0,0)+\sum_{(k_1,k_2)\neq(m,n),(i,j)}a_{(i,j),(k_1,k_2)}[h_{k_1,k_2}(0)-h_{i,j}(0)],$$

$$\begin{aligned}\Delta_{i,j}^{(\ell)}=&f_{i,j}(0,0)-f_{i,j}(\tilde{x}_{i,j}^{(\ell)},\tilde{y}_{i,j}^{(\ell)})\\&+a_{(i,j),(m,n)}[h_{m,n}(\eta_{m,n}^{(\ell)})-h_{m,n}(\tilde{x}_{m,n}^{(\ell)})-h_{i,j}(0)+h_{i,j}(\tilde{x}_{i,j}^{(\ell)})]\\&+\sum_{(k_1,k_2)\neq(m,n),(i,j)}a_{(i,j),(k_1,k_2)}[h_{k_1,k_2}(0)-h_{k_1,k_2}(\tilde{x}_{k_1,k_2}^{(\ell)})\\&-h_{i,j}(0)+h_{i,j}(\tilde{x}_{i,j}^{(\ell)})].\end{aligned}$$

Subtracting Eq. (38) for $\ell=1$ from that for $\ell=2$ yields $\forall(i,j)\neq(m,n)$,

$$a_{(i,j),(m,n)}v_{m,n}+e_{(i,j),(m,n)}=\theta d_{(i,j),(m,n)}, \tag{39}$$

where

$$v_{m,n}=h_{m,n}(\eta_{m,n}^{(2)})-h_{m,n}(\eta_{m,n}^{(1)}),$$

$$e_{(i,j),(m,n)}=\Delta_{i,j}^{(1)}-\Delta_{i,j}^{(2)},$$

$$d_{(i,j),(m,n)}=\tilde{x}_{i,j}^{(2)}-\tilde{x}_{i,j}^{(1)}.$$

It follows

$$\theta d_{(i,j),(m,n)}=\begin{cases}e_{(i,j),(m,n)}, & \text{for } a_{(i,j),(m,n)}=0\\ v_{m,n}+e_{(i,j),(m,n)}, & \text{for } a_{(i,j),(m,n)}=1\end{cases}, \tag{40}$$

which implies that all values $|\theta d_{(i,j),(m,n)}|$ can be divided into two sets: $\mathbf{I}_0$ containing all elements $|\theta d_{(i,j),(m,n)}|$ corresponding to $a_{ij}=0$ and $\mathbf{I}_1$ containing all elements $|\theta d_{(i,j),(m,n)}|$ corresponding to $a_{ij}=1$. Therefore, if one can distinguish the sets $\mathbf{I}_0$ and $\mathbf{I}_1$ then one can identify the parameters $a_{(i,j),(m,n)}$.

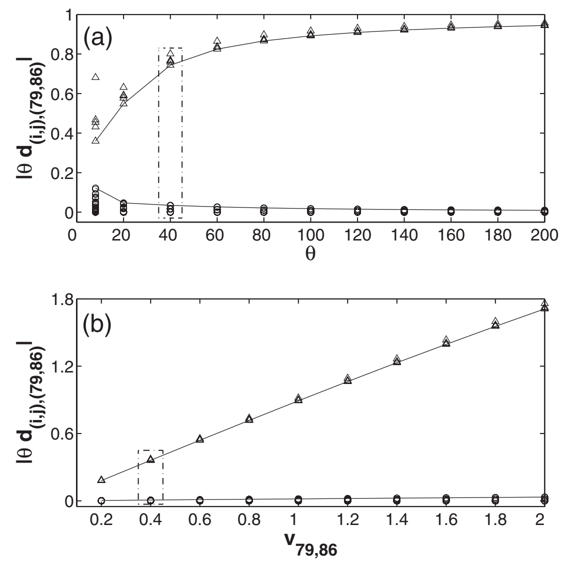

FIG. 5. Estimation of connections starting from site (79,86) as a representative site of the FHN medium [Eqs. (26)–(30)] with additional remote connections shown in Fig. 2(a) where there exist five connections starting from site (79,86), including four nearest neighbor connections plus the remote linkage from site (79,86) to site (14,40). (a) For each θ, we plot $|\theta d_{(i,j),(79,86)}|$ vertically, as shown in the dashed frame for $\theta=40$, where the quantity being plotted in vertical axis has arbitrary unit but that in the horizontal axis has no unit; (b) For each $v_{79,86}$, we plot $|\theta d_{(i,j),(79,86)}|$ vertically, as shown in the dashed frame for $v_{79,86}=0.4$, where the unit of the quantity being plotted in each axis is arbitrary. There the values $|\theta d_{(i,j),(79,86)}|$ corresponding to $a_{(i,j),(79,86)}=1$ and those corresponding to $a_{(i,j),(79,86)}=0$ are plotted with $\triangle$ and $\bigcirc$, respectively; the upper and lower solid lines are formed by linking all critical points of the sets $\mathbf{I}_1$ and $\mathbf{I}_0$, respectively.

As shown in Sec. II D, there exists a critical value θ_c [36] such that if $\theta>\theta_c$, then one may distinguish both sets $\mathbf{I}_0$ and $\mathbf{I}_1$ since, in this case, the distance between the sets $\mathbf{I}_0$ and $\mathbf{I}_1$ is larger than the maximal value of set $\mathbf{I}_0$. This is illustrated in Fig. 5(a) where $\theta_c\approx 7.5$. Furthermore, the maximal value of set $\mathbf{I}_0$ ($\bigcirc$) decreases with θ and the minimal value of set $\mathbf{I}_1$ ($\triangle$) increases with θ. The performance of topology identification also depends on the value of $v_{(m,n)}$. In particular, both the minimal value of set $\mathbf{I}_1$ and the maximal value of set $\mathbf{I}_0$ increase almost linearly with $v_{(m,n)}$, but the latter has much bigger increasing rate than the former, as illustrated in Fig. 5(b) where $\theta=100$. All above features may be applied to discriminate the sets $\mathbf{I}_0$ and $\mathbf{I}_1$.

IV. DISCUSSION

The suggested topology estimation method is applicable to any spatially extended system (including unbalanced systems). For unbalanced systems, the term $-\Sigma_{i,j}D_{i,j}$ will appear in the right-hand side of Eq. (36) and distort the estimation of function $f_{i,j}+\Gamma$. In this case, if there exists a balanced subnetwork containing the element (i,j), Eq. (36) may still be used to estimate $f_{i,j}+\Gamma$ by driving the balanced subnetwork to steady states, where the summation in the right-hand side of Eq. (36) is over only the elements of the balanced subnetwork.

It should be remarked that the suggested topology estimation method is applicable to weighted systems [Eqs. (26)–(28)] where $a_{(i,j),(k_1,k_2)}>0$ if there exists a connection from site (k_1,k_2) to site (i,j), and $a_{(i,j),(k_1,k_2)}=0$ otherwise. Indeed, in this case, the value of $v_{m,n}$ in Eq. (39) reads $v_{m,n}=a_{(i,j),(m,n)}[h_{m,n}(\eta^{(2)}_{m,n})-h_{m,n}(\eta^{(1)}_{m,n})]$. Again, one may identify the connections starting from site (m,n) by distinguishing sets $\mathbf{I}_0$ (containing all elements $|\theta d_{(i,j),(m,n)}|$ corresponding to $a_{ij}=0$) and $\mathbf{I}_1$ (containing all elements $|\theta d_{(i,j),(m,n)}|$ corresponding to $a_{ij}>0$). However, one in general cannot identify the values of parameters $a_{(i,j),(k_1,k_2)}$ themselves.

We have introduced a control based method to system identification of spatially extended systems and networks with inhomogeneous local dynamics and additional long-range connection topology and with any boundary and initial conditions. The method is applicable if the required observables are available and if the system can be stabilized to a steady state. If stabilizing the full system is not possible, a sequence of measurements may be performed where only small regions are stabilized and the remaining system is not controlled. In this way the whole system structure can be identified by collecting and combining information obtained from many small regions. The required effort to apply the control based identification method depends on the size of the full system, the size (and number) of local regions where control is applied (potentially in parallel), the transient time until the controlled region is at the steady state, and the noise level (if the noise is too strong one has to repeat measurements).

We demonstrated here the suggested identification method for extended systems given by coupled ODEs. Such systems of ODEs may be the result of some discrete physical description (for example, on a cell level) or be the result of an approximation [27] of some underlying PDE. In this sense control based identification provides a general tool for coping with inhomogeneous systems with (partially) unknown dynamics and possible long-range interaction links.

ACKNOWLEDGMENTS

This work was partially supported by the National Natural Science Foundation of China under Grants No. 10602026, No. 60934002, and No. 60973118, and by the Outstanding Youth Foundation of Sichuan Province under Grant No. 2010JQ0001. The authors thank L. Kocarev for his helpful discussions. U.P. acknowledges financial support from the Max Planck Society (research contract "Analyse biophysikalischer Daten") and the Bernstein Center for Computational Neuroscience (BCCN) Goettingen (project D1).

[1] *Chemical Waves and Patterns*, edited by R. Kapral and K. Showalter (Kluwer, Dordrecht, The Netherlands, 1995).
[2] A. T. Winfree, *The Geometry of Biological Time* (Springer, New York, 2000).
[3] T. G. Müller and J. Timmer, Int. J. Bifurcation Chaos Appl. Sci. Eng. **14**, 2053 (2004).
[4] L. Guo and S. A. Billings, IEEE Trans. Circuits Syst., II: Express Briefs **53**, 657 (2006).
[5] U. Parlitz and C. Merkwirth, Phys. Rev. Lett. **84**, 1890 (2000).
[6] S. Mandelj, I. Grabec, and E. Govekar, Int. J. Bifurcation Chaos Appl. Sci. Eng. **14**, 2011 (2004).
[7] D. Napoletani and T. D. Sauer, Phys. Rev. E **77**, 026103 (2008).
[8] T. S. Gardner, D. di Bernardo, D. Lorenz, and J. J. Collins, Science **301**, 102 (2003).
[9] B. N. Kholodenko, A. Kiyatkin, F. J. Bruggeman, E. Sontag, H. V. Westerhoff, and J. B. Hoek, Proc. Natl. Acad. Sci. U.S.A. **99**, 12841 (2002).
[10] M. Timme, Phys. Rev. Lett. **98**, 224101 (2007).
[11] L. Junge and U. Parlitz, Phys. Rev. E **61**, 3736 (2000).
[12] D. Yu, M. Righero, and L. Kocarev, Phys. Rev. Lett. **97**, 188701 (2006).
[13] G. S. Duane, D. Yu, and L. Kocarev, Phys. Lett. A **371**, 416 (2007).
[14] H. D. I. Abarbanel, D. R. Creveling, and J. M. Jeanne, Phys. Rev. E **77**, 016208 (2008).
[15] V. Braitenberg and A. Schütz, *Cortex: Statistics and Geometry of Neuronal Connectivity*, 2nd ed. (Springer-Verlag, Heidelberg, 1998).
[16] G. Buzsáki, C. Geisler, D. A. Henze, and X.-J. Wang, Trends Neurosci. **27**, 186 (2004).
[17] M. A. Dahlem, F. M. Schneider, and E. Schöll, Chaos **18**, 026110 (2008).
[18] W. D. Kepseu and P. Woafo, Phys. Rev. E **78**, 011922 (2008).
[19] H. Sakaguchi and P. Woafo, Phys. Rev. E **77**, 042902 (2008).
[20] A. Roxin, H. Riecke, and S. A. Solla, Phys. Rev. Lett. **92**, 198101 (2004).
[21] D. He, G. Hu, M. Zhan, W. Ren, and Z. Gao, Phys. Rev. E **65**, 055204 (2002).
[22] X. Wang, Y. Lu, M. Jiang, and Q. Ouyang, Phys. Rev. E **69**, 056223 (2004).
[23] S. Sinha, J. Saramäki, and K. Kaski, Phys. Rev. E **76**, 015101 (2007).
[24] I. Z. Kiss, Y. Zhai, and J. L. Hudson, Phys. Rev. Lett. **88**, 238301 (2002).
[25] W. Wang, I. Z. Kiss, and J. L. Hudson, Phys. Rev. Lett. **86**, 4954 (2001).
[26] K. Karahaliloglu and S. Balkir, Int. J. Circuit Theory Appl. **31**, 571 (2003).
[27] http://www.scholarpedia.org/article/Method_of_lines
[28] M.-J. Chien, IEEE Trans. Circuits and Systems-I **CAS–32**, 655 (1976).
[29] R. O. Grigoriev, M. C. Cross, and H. G. Schuster, Phys. Rev. Lett. **79**, 2795 (1997).
[30] N. Parekh, S. Parthasarathy, and S. Sinha, Phys. Rev. Lett. **81**, 1401 (1998).
[31] K. Pyragas, Phys. Lett. A **170**, 421 (1992).
[32] A. Ahlborn and U. Parlitz, Phys. Rev. Lett. **93**, 264101 (2004).

[33] Here and hereafter the distance between two point sets is equal to the minimal distance between any two points which are taken from different sets.

[34] We suggest here only a five-point Laplacian approximation. One could also use a higher order one (e.g., nine-point Laplacian operator).

[35] If only Γ is unknown, then one may follow the methods introduced in Sec. II C for estimating the value of Γ.

[36] In practice, one can first choose a small gain θ and then increase θ gradually until the distance between the sets $\mathbf{I}_0$ and $\mathbf{I}_1$ is larger than the maximal value of set $\mathbf{I}_0$ and thus the sets $\mathbf{I}_0$ and $\mathbf{I}_1$ are distinguishable. In this way, one may determine the critical value θ_c.